A Molecular Classification of Papillary Renal Cell Carcinoma

Ximing J. Yang,[1,2] Min-Han Tan,[5,12,13] Hyung L. Kim,[8] Jonathon A. Ditlev,[5] Mark W. Betten,[5] Carolina E. Png,[5] Eric J. Kort,[5] Kunihiko Futami,[5] Kyle A. Furge,[6] Masayuki Takahashi,[5,10] Hiro-omi Kanayama,[10] Puay Hoon Tan,[11] Bin Sing Teh,[14] Chunyan Luan,[1] Kim Wang,[1] Michael Pins,[1] Maria Tretiakova,[3] John Anema,[7] Richard Kahnoski,[7] Theresa Nicol,[16] Walter Stadler,[4] Nicholas G. Vogelzang,[18] Robert Amato,[15] David Seligson,[9] Robert Figlin,[8] Arie Belldegrun,[8] Craig G. Rogers,[17] and Bin Tean Teh[5]

Departments of [1]Pathology and [2]Urology, Feinberg School of Medicine, Northwestern University; Department of [3]Pathology and [4]Medical Oncology, University of Chicago, Chicago, Illinois; [5]Laboratory of Cancer Genetics and [6]Bioinformatics Program, Van Andel Research Institute; [7]Department of Urology, Spectrum Health Hospital, Grand Rapids, Michigan; Departments of [8]Urology and [9]Pathology, University of California, Los Angeles, California; [10]Department of Urology, University of Tokushima, Tokushima, Japan; [11]Department of Pathology, Singapore General Hospital; [12]Department of Medical Oncology, National Cancer Center; [13]Department of Medicine, Alexandra Hospital, Singapore, Singapore; [14]Department of Radiation Oncology, Baylor College of Medicine and The Methodist Hospital; [15]Genitourinary Oncology Program, The Methodist Hospital, Houston, Texas; Departments of [16]Pathology and [17]Urology, Johns Hopkins University, Baltimore, Maryland; and [18]Department of Medical Oncology, Nevada Cancer Institute, Reno, Nevada

Abstract

Despite the moderate incidence of papillary renal cell carcinoma (PRCC), there is a disproportionately limited understanding of its underlying genetic programs. There is no effective therapy for metastatic PRCC, and patients are often excluded from kidney cancer trials. A morphologic classification of PRCC into type 1 and 2 tumors has been recently proposed, but its biological relevance remains uncertain. We studied the gene expression profiles of 34 cases of PRCC using Affymetrix HGU133 Plus 2.0 arrays (54,675 probe sets) using both unsupervised and supervised analyses. Comparative genomic microarray analysis was used to infer cytogenetic aberrations, and pathways were ranked with a curated database. Expression of selected genes was validated by immunohistochemistry in 34 samples with 15 independent tumors. We identified two highly distinct molecular PRCC subclasses with morphologic correlation. The first class, with excellent survival, corresponded to three histologic subtypes: type 1, low-grade type 2, and mixed type 1/low-grade type 2 tumors. The second class, with poor survival, corresponded to high-grade type 2 tumors (n = 11). Dysregulation of G_1-S and G_2-M checkpoint genes were found in class 1 and 2 tumors, respectively, alongside characteristic chromosomal aberrations. We identified a seven-transcript predictor that classified samples on cross-validation with 97% accuracy. Immunohistochemistry confirmed high expression of cytokeratin 7 in class 1 tumors and of topoisomerase IIα in class 2 tumors. We report two molecular subclasses of PRCC, which are biologically and clinically distinct and may be readily distinguished in a clinical setting. (Cancer Res 2005; 65(13): 5628-37)

Introduction

Kidney cancer is a heterogenous disease consisting of various subtypes with diverse genetic, biochemical, and morphologic features. Epithelial renal cell carcinoma (RCC) accounts for the vast majority of renal malignancies in adults. Based on morphologic features defined in the WHO International Histological Classification of Kidney Tumors, RCC can be divided into clear cell (conventional), papillary (chromophil), chromophobe, collecting duct, and unclassified subtypes (1, 2). Papillary RCC (PRCC) is the second most common subtype comprising 10% to 15% of kidney cancers (3), with an estimated annual incidence of between 3,500 and 5,000 cases in the United States, based on overall statistics for kidney cancer (4). PRCC is histologically characterized by the presence of fibrovascular cores with tumor cells arranged in a papillary configuration. The majority of PRCC tumors show indolent behavior and have a limited risk of progression and mortality, but a distinct subset displays highly aggressive behavior (5). The biological and clinical aspects of this cancer have been reviewed recently (6).

Delahunt and Eble have proposed that PRCC can be morphologically classified into two subtypes (7). Type 1 is characterized by the presence of small cuboidal cells covering thin papillae, with a single line of small uniform nuclei and basophilic cytoplasm. Type 2 is characterized by the presence of large tumor cells with eosinophilic cytoplasm and pseudostratification. Generally, type 2 tumors have a poorer prognosis than type 1 tumors (8). However, the morphologic classification remains controversial, and there is limited molecular and biochemical evidence to support this morphologic classification. The relatively high incidence of mixed type 1 and 2 tumors poses additional difficulties for such a method of classification. As a result, some recent studies of PRCC do not stratify PRCC into type 1 and 2 tumors (9, 10).

Despite the moderate incidence of PRCC, comparable with that of chronic myeloid leukemia, there is a disproportionately limited knowledge about the underlying molecular basis for development and progression of PRCC. To date, no effective therapy is available for patients with advanced PRCC (11), and patients with PRCC may be excluded from clinical trials that are usually designed for the more common clear cell RCC. It is thus imperative to identify new molecular markers for establishing an accurate diagnosis and prognosis and for developing effective medical therapies for this cancer. Gene expression profiling is a technique that has shown promise in addressing these issues in RCC (12). Recently, we and several other groups of investigators have reported molecular signatures specific for several subtypes of kidney cancer, including PRCC (13–18). PRCC can be effectively distinguished from the other major subtypes of RCC using gene classifiers, from which

Note: Supplementary data for this article are available at Cancer Research Online (http://cancerres.aacrjournals.org/).

X.J. Yang and M-H. Tan contributed equally to this work.

Requests for reprints: Bin Tean Teh, 333 Bostwick Avenue Northeast, Grand Rapids, MI 49503. Phone: 616-234-5350; Fax: 616-234-5115; E-mail: bin.teh@vai.org.

Table 1. Clinicopathologic features with molecular classification

Patient ID	Age (y)	Gender	Histologic classification (type)	Molecular classification (class)	Size (cm)	Tumor-node-metastasis stage	M stage	Grade	Patient status*	Survival (mo)
P01	46	F	2B	2	15.2	4	1	3	NA	NA
P02	59	M	1	1	4.5	1	X	1	NA	NA
P03	68	M	1	1	4	1	X	2	NA	NA
P04	32	M	2A	1	7	1	X	2	NA	NA
P05	71	M	1 and 2A	1	4.7	1	0	2	DOO	30
P06	70	M	1	1	1.2	3	0	2	NED	26
P07	72	F	1	1	3	1	0	2	DOO	8
P08	73	F	1	1	3	1	0	2	NED	25
P09	84	F	1	1	3.5	1	0	2	NED	27
P10	56	F	1	1	14	3	0	2	NED	13
P11	56	M	1	1	3.5	1	0	2	NED	13
P12	80	F	1	1	2.5	1	0	2	NED	4
P13	64	M	1	1	5.5	1	0	2	DOD	74
P14	44	M	1	1	3.5	3	0	2	NED	95
P15	76	M	1 and 2A	1	4.5	1	0	2	NED	58
P16	72	M	2B	2	10	3	0	4	DOD	17
P17	55	M	1	1	5	3	0	2	NED	30
P18	71	F	2B	2	3	1	0	3	NED	32
P19	76	M	2B	2	5.7	3	0	3	NED	36
P20	71	M	1	1	2.7	1	0	2	DOO	63
P21	80	F	2A	1	3.5	2	0	2	NED	66
P22	53	M	1 and 2A	1	2.3	1	0	2	NED	61
P23	54	M	2B	2	8	4	0	4	DOD	12
P24	50	M	2B	2	11	3	1	3	DOO	37
P25	44	M	2B	2	14	4	1	4	AWC	12
P26	75	M	2A	1	9	2	0	2	NA	NA
P27	74	M	1 and 2A	1	6	1	0	2	NED	24
P28	37	M	1 and 2A	1	6	1	0	2	DOO	12
P29	43	M	1	1	5	1	0	2	NA	NA
P30	63	M	2A	2	6.9	3	0	2	DOO	34
P31	62	M	2B	2	6.8	4	1	3	DOO	4
P32	56	M	2B	2	6	4	1	3	DOD	16
P33	71	F	2B	2	15	4	1	3	DOD	29
P34	49	F	2B	2	15	4	1	3	DOD	9

*Last known status: DOD, died of disease; DOO, died of other causes; AWC, alive with cancer; NED, no evidence of disease.

α-methylacyl-CoA racemase has been additionally validated as a useful immunohistochemical marker (19). However, no distinct molecular subclasses of PRCC were identified in any study possibly because of limited numbers of tumors in previous expression studies (between 2 and 9). We therefore did gene expression profiling on 34 cases of PRCC to search for distinct molecular subtypes of PRCC that were both biologically and clinically relevant.

Materials and Methods

Patient samples and tissue processing. Institutional review board approval was obtained from each participating institution. Frozen samples of 43 primary tumor specimens with a diagnosis of PRCC after routine pathologic review at each medical center were initially collected following nephrectomy. All tumor specimens were collected from participating institutions in the United States, except one case from Japan. Tumor tissue was flash frozen in liquid nitrogen immediately after nephrectomy and stored at −80°C. Portions of the tumors were fixed in buffered formalin, and H&E-stained slides for all cases were centrally reviewed, except for one case (P30), where slides were not available and histologic description from the pathology report was used for subclassification. We extracted total RNA from homogenized samples using Trizol reageant (Invitrogen, Carlsbad, CA) as described previously. Total RNA was subsequently purified with a RNeasy kit (Qiagen, Montgomery County, MD), and quality was assessed on denaturing gel electrophoresis. Nine specimens were excluded because of degraded RNA quality. Information on metastatic status at surgery was derived by review of pathologic, radiologic, and intraoperative findings. Clinicopathologic features of the final 34 cases have been provided in Table 1. Twelve noncancerous kidney cortical specimens were also obtained for comparison of gene expression profiling. For histologic evaluation and immunohistochemical analysis, formalin-fixed, paraffin-embedded tissue blocks and sections were obtained from a total of 34 cases. Nineteen of these cases had undergone expression profiling and the additional 15 cases were derived from independent patients, whom did not have tumor tissue profiled.

Expression profiling. For oligonucleotide expression profiling, total RNA (5-20 μg) was used to prepare antisense biotinylated RNA. A subset of cases was added to external poly(A) RNA-positive controls (Affymetrix, Santa Clara, CA). Synthesis of single-stranded and double-stranded cDNA was done with the use of T7-oligo(dT) primer (Affymetrix). *In vitro* transcription

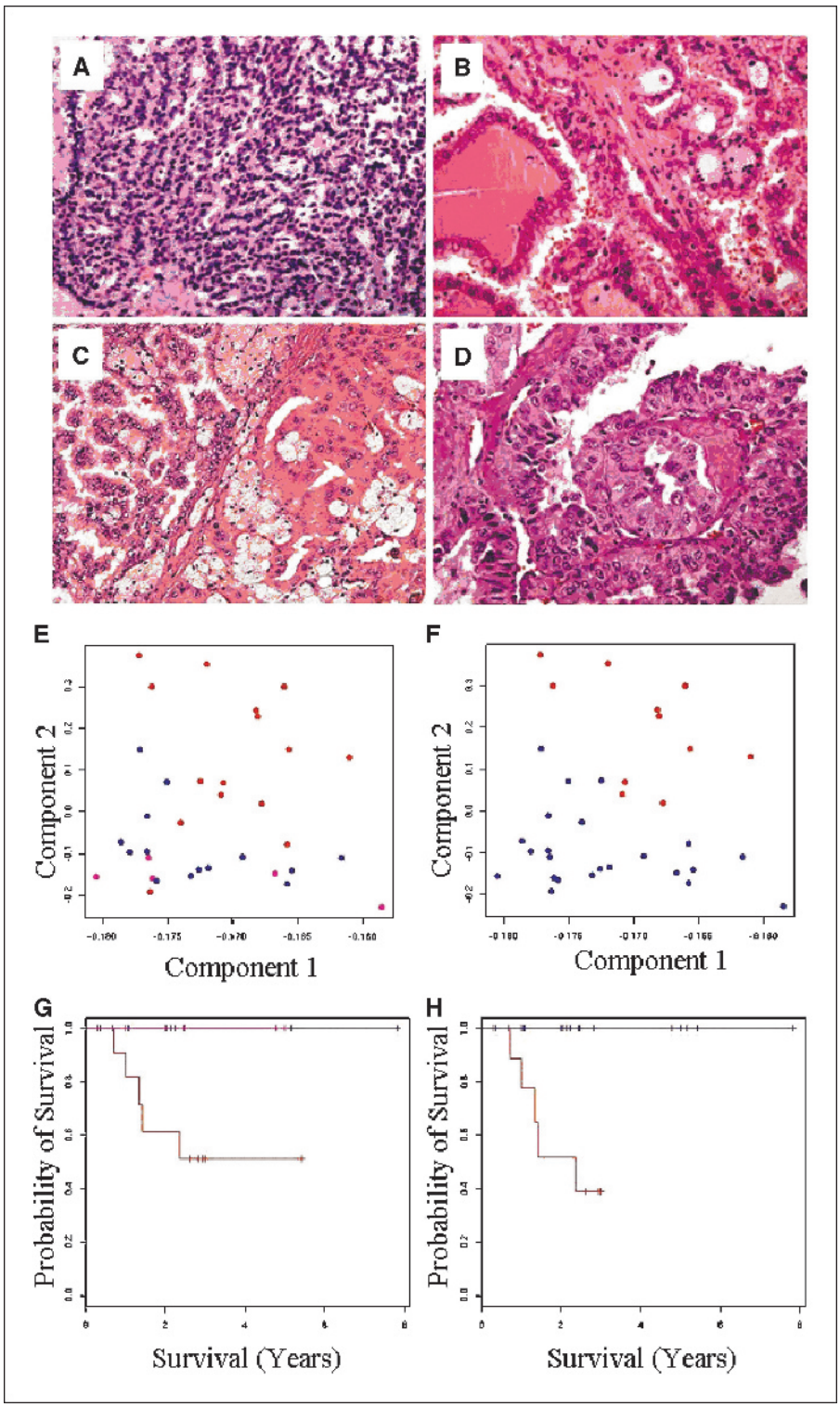

Figure 1. Classification of PRCC by histology, expression profiling, and survival. *A,* type 1 PRCC (class 1) with basophilic cytoplasm (Fuhrman grade 2). *B,* type 2A PRCC (class 1) with eosinophilic cytoplasm (Fuhrman grade 2). *C,* mixed type 1 and 2A PRCC (class 1) with combined type 1 (*left*) and type 2A (*right*) components (Fuhrman grade 2). *D,* type 2B PRCC (class 2) with eosinophilic cytoplasm and pseudostratified layers of tumor cells (Fuhrman grade 3). *E,* visualization of expression profiles by first two principal components grouped into type 1 (*blue*), type 2 (*red*), and mixed type 1/2 (*pink*) tumors. *F,* visualization of expression profiles by first two principal components grouped into class 1 (*blue*) and class 2 (*red*) tumors. *G,* survival analysis of type 1 (*blue*), type 2 (*red*), and mixed type 1/2 (*pink*) tumors. Type 1 and mixed type 1/2 tumors have overlapping curves. *H,* survival analysis of class 1 (*blue*) and class 2 (*red*) tumors.

was done using Enzo Bioarray Transcript Labeling kit (Enzo, Farmingdale, NY). The biotinylated cRNA was subsequently fragmented, and 10 μg were hybridized to each array at 45°C over 16 hours. The HGU133 Plus 2.0 GeneChips contain 54,675 probe sets, representing ~47,000 transcripts and variants. Scanning was done in a GeneChip 3000 scanner. Quality assessment was done in GeneChip Operating System 1.1.1 (Affymetrix) using global scaling to a target signal of 500. Quality assessment was done using denaturing gel electrophoresis. The manufacturer's recommended protocol (GeneChip Expression Analysis Technical Manual, Affymetrix, April 2003) was followed for expression profiling. Median background was 73, median scaling factor was 3.06, and median *GADPH* 3′/5′ ratio was 1.03, indicative of a high overall array and RNA quality. The data discussed in this publication have been deposited in NCBI's Gene Expression Omnibus (GEO)[19] and are accessible through GEO Series Accession number GSE2748.

[19] http://www.ncbi.nlm.nih.gov/geo/.

Table 2. Histologic subclassification

Type	Cell size	Cytoplasm	Grade	Molecular classification (class)
1	Small	Pale	1-2	1
1 and 2A	Small/large	Pale/eosinophilic	1-2	1
2A	Large	Eosinophilic	1-2	1
2B	Large	Eosinophilic	3-4	2

Data analysis. Statistical analyses were done in the statistical environment R 2.0.1 using packages from the Bioconductor project (20). The robust multichip average algorithm was used to perform preprocessing of the CEL files, including background adjustment, quartile normalization, and summarization. Principal component analysis was used to visualize the 34 expression profiles. Significance analysis of microarrays (SAM) based on two-class unpaired analysis, assumption of unequal group variances, and 10,000 permutations was used to derive a list of genes differentially expressed between tumor subclasses and ordered by relative fold change (21). We did pathway analysis on these genes using Ingenuity Pathway Analysis (Ingenuity Systems, Mountain View, CA), and enrichment of canonical pathways was assessed for significance by a hypergeometric algorithm that did not correct for multiple testing. For derivation of a small gene classifier, we used prediction analysis of microarrays (PAM), a *R* implementation of nearest shrunken centroids methodology with 10-fold cross-validation over 30 gene thresholds and an offset percentage of 30% (22). Gene predictors corresponding to a minimum misclassification error were obtained, with class discriminant scores calculated for class 1 and 2 tumors as described previously. We inferred cytogenetic profiles for the tumors through the use of a refinement of the comparative genomic microarray analysis (CGMA) algorithm (23), which predicts chromosomal alterations based on regional changes in expression. Relative expression profiles (R) were generated from the single-channel tumor expression profiles (T) and the mean expression values of the 12 single-channel kidney cortical expression profiles (N), such that $R = \log_2(T) - \log_2(N)$. Survival analysis was done by fitting to a Cox proportional hazards model, and significance was determined by the likelihood ratio test. Two-tailed Student's t test and Fisher's exact testing was used to evaluate correlation between variables and tumor subclassification. For the purpose of this analysis, tumor grade and stage was classified into two categories corresponding to low grade or stage (1 and 2) versus high grade and stage (3 and 4).

Immunohistochemistry. Immunostaining was done on 5 μm thick formalin-fixed, paraffin-embedded sections using the biotin-avidin system (19) with mouse monoclonal antibodies specific for cytokeratin 7 (CK7; 1:50 dilution, DAKO, Carpinteria, CA) and DNA topoisomerase IIα (TopIIα; 1:20 dilution, Vector Laboratories, Burlingame, CA) as described previously. To verify the differential value of CK7 and TopIIα, we studied 19 PRCC samples that had undergone microarray analysis (10 class 1 tumors and 5 class 2 tumors) as well as an independent set of 15 tumors (10 class 1 tumors and 5 class 2 tumors). The 21 class 1 tumors were composed of histologic type 1 (n = 15), low-grade type 2 tumors (n = 3), and mixed type 1/low-grade type 2 tumors (n = 8). The 13 class 2 tumors were all high-grade type 2 tumors. The CK7 immunoreactivity was graded as negative (<0.1% positive tumor cells), focally positive (0.1-10% positive tumor cells), or positive (>10% positive tumor cells). The TopIIα immunoreactivity was graded as negative (<0.1% positive tumor cells), focally positive (0.1-10% positive tumor cells), or positive (>10% positive tumor cells). The Mann-Whitney test was used to evaluate significance of the differential staining.

Results

Morphologic characteristics. Based on histologic features and Fuhrman grading system, we designated four categories of tumors: type 1 (n = 14; Fig. 1*A*) characterized by small tumor cells of low Fuhrman grade (≤2); type 2A (n = 4; Fig. 1*B*) characterized by large eosinophilic tumor cells of low Fuhrman grade (≤2); combined type 1 and 2A (n = 5; Fig. 1*C*); and type 2B (n = 11; Fig. 1*D*) characterized by large eosinophilic tumor cells with Fuhrman grade (≥3; Table 2).

Molecular characteristics. We visualized the 34 expression profiles by principal component analysis. We noted overlap between histologic type 1 and 2 tumors, contrary to our expectation of distinct molecular subtypes (Fig. 1*E*). Tumors with mixed type 1 and 2 components (n = 5) grouped with type 1 tumors. PAM with 10-fold cross-validation persistently classified three of four low-grade type 2 tumors with type 1 tumors over a wide range of shrinking gene thresholds (Supplementary Fig. S1A). The only low-grade type 2 tumor that persistently classified with the high-grade type 2 tumors was P30 (the only tumor we were unable to personally evaluate histologically to confirm a reported grade of 2). These results supported a hypothesis that type 2 tumors were molecularly heterogenous. We analyzed the profiles based on this morphologic subtyping into two classes (class 1 corresponding to type 1, low-grade type 2, and mixed type 1/low-grade type 2 tumors and class 2 corresponding to high-grade type 2 tumors) from a molecular viewpoint. Visualization of principal components now showed distinct differentiation between expression profiles of class 1 and 2 tumors, consistent with distinct tumor subclasses (Fig. 1*F*). Transcripts (n = 796) differentially expressed between class 1 and 2 tumors were identified using SAM at a δ of 1.8, with a false discovery rate of 0.01. We list the top 50 transcripts relatively upexpressed in each subclass (Table 3) and show a hierarchical clustering of the tumor samples based on these 100 transcripts (Fig. 2*A*). We were able to identify multiple gene classifiers that effectively differentiated class 1 and 2 tumors at 97% accuracy at multiple shrinkage thresholds using PAM (between 7 and 3,881 transcripts) using nearest shrunken centroids methodology (Supplementary Fig. S1B). We report here the seven-transcript predictor that achieved this accuracy (Table 4). Only the tumor of P30, initially reported as a type 2 tumor with grade 2, which we were unable to confirm histologically, persistently classified as a class 2 tumor, rather than as a class 1 tumor, throughout these multiple shrinkage thresholds.

Survival characteristics. Survival analysis (Fig. 1*G* and *H*) showed that this refined morphologic and molecular classification system showed a survival prediction that showed a statistically insignificant edge over the previous morphology-based classification approach (Nagelkerke's $R^2 = 0.505$ and $P = 0.001$ versus $R^2 = 0.389$ and $P = 0.005$). Class 2 tumors were larger in tumor dimension (P = 0.003), of higher grade ($P < 0.001$), of higher stage ($P < 0.001$), and were more likely to exhibit distant metastases at initial surgery (P < 0.001) than class 1 tumors. Indeed, all tumors metastatic at initial surgery were class 2 tumors (n = 7). No significant difference in age (P = 0.37) or gender (P = 0.70) was found between the two classes.

Chromosomal aberrations inferred by comparative genomic microarray analysis. Distinct cytogenetic profiles for each tumor were generated using high-resolution CGMA (Fig. 2*B*). Full-length gains in chromosomes 7, 12, 16, 17, and 20 was found both in class 1 and 2 tumors, consistent with the previously reported trisomies observed by using conventional cytogenetic analysis characteristic of PRCC (24, 25). However, in comparison with class 1 tumors, class 2 tumors exhibited more frequent gains at 1q, 2, and 8q and losses at 3p and 6q and showed fewer gains of chromosome 3, 7, and 16. More frequent losses of 6q and 14q were also evident.

Pathway analysis. Genes (n = 203) derived from the 796 transcripts were eligible for generation of networks in pathway

Table 3. Top 100 differentially expressed genes in class 1 and 2 PRCC

Probe ID	Gene description	$D(i)^*$	SD	P	Q	Fold change [†]
Genes upexpressed in class 1 PRCC						
213456_at	*Sclerostin domain-containing 1*	−7.2	0.5	0.0	0.0	33.4
201539_s_at	*Four and a half LIM domains 1*	−10.9	0.3	0.0	0.0	14.8
204304_s_at	*Prominin 1*	−8.0	0.6	0.0	0.0	14.4
210298_x_at	*Four and a half LIM domains 1*	−9.9	0.4	0.0	0.0	14.3
214505_s_at	*Four and a half LIM domains 1*	−11.3	0.3	0.0	0.0	12.1
210299_s_at	*Four and a half LIM domains 1*	−8.1	0.5	0.0	0.0	10.6
209016_s_at	*Keratin 7*	−6.9	0.5	0.0	0.0	8.4
205597_at	*Chromosome 6 open reading frame 29*	−11.4	0.3	0.0	0.0	8.3
232151_at	*mRNA full-length insert cDNA clone EUROIMAGE 2344436*	−9.2	0.4	0.0	0.0	8.0
1566764_at	*mRNA full-length insert cDNA clone EUROIMAGE 2344436*	−8.0	0.4	0.0	0.0	7.5
1553809_a_at	*Chromosome 9 open reading frame 71*	−6.9	0.3	0.0	0.0	6.5
1566766_a_at	*mRNA full-length insert cDNA clone EUROIMAGE 2344436*	−10.0	0.3	0.0	0.0	6.0
224027_at	*Chemokine (C-C motif) ligand 28*	−7.2	0.3	0.0	0.0	5.7
1555203_s_at	*Chromosome 6 open reading frame 29*	−9.7	0.2	0.0	0.0	5.3
238184_at	*Transcribed sequences*	−9.4	0.2	0.0	0.0	4.8
202820_at	*Aryl hydrocarbon receptor*	−7.2	0.3	0.0	0.0	4.2
202790_at	*Claudin 7*	−9.1	0.2	0.0	0.0	4.0
222764_at	*Asparaginase-like 1*	−8.1	0.2	0.0	0.0	3.9
219127_at	*Hypothetical protein MGC11242*	−7.5	0.2	0.0	0.0	3.6
218857_s_at	*Asparaginase-like 1*	−9.0	0.2	0.0	0.0	3.5
229084_at	*Contactin 4*	−6.9	0.2	0.0	0.0	3.4
219614_s_at	*Solute carrier family 6 (neurotransmitter transporter), member 20*	−10.1	0.2	0.0	0.0	3.2
210398_x_at	*Fucosyltransferase 6 [α(1,3) fucosyltransferase]*	−8.3	0.2	0.0	0.0	3.1
205405_at	*Semaphorin 5A*	−7.3	0.2	0.0	0.0	3.0
1559361_at	*mRNA full-length insert cDNA clone EUROIMAGE 2344436*	−8.2	0.2	0.0	0.0	2.8
203365_s_at	*Matrix metalloproteinase 15 (membrane-inserted)*	−10.0	0.1	0.0	0.0	2.6
229144_at	*KIAA1026 protein*	−7.9	0.2	0.0	0.0	2.4
211110_s_at	*Androgen receptor*	−6.9	0.2	0.0	0.0	2.3
223636_at	*Zinc finger, MYND domain-containing 12*	−7.5	0.1	0.0	0.0	2.2
231022_at	*Transcribed sequences*	−7.0	0.2	0.0	0.0	2.2
221665_s_at	*EPS8-like 1*	−8.0	0.1	0.0	0.0	2.1
235937_at	*Occluding*	−7.1	0.1	0.0	0.0	2.1
217795_s_at	*Hypothetical protein MGC3222*	−7.5	0.1	0.0	0.0	2.1
211621_at	*Androgen receptor*	−7.3	0.1	0.0	0.0	2.1
210399_x_at	*Fucosyltransferase 6 [α(1,3) fucosyltransferase]*	−7.1	0.1	0.0	0.0	2.0
202005_at	*Suppression of tumorigenicity 14 (colon carcinoma, matriptase, epithin)*	−7.1	0.1	0.0	0.0	1.9
243225_at	*Hypothetical protein LOC283481*	−7.2	0.1	0.0	0.0	1.9
91826_at	*EPS8-like 1*	−8.2	0.1	0.0	0.0	1.7
218779_x_at	*EPS8-like 1*	−7.5	0.1	0.0	0.0	1.7
205977_s_at	*EphA1*	−9.1	0.1	0.0	0.0	1.6
235293_at	*cDNA FLJ45593 fis, clone BRTHA3014920*	−7.5	0.1	0.0	0.0	1.6
238028_at	*Similar to hypothetical protein BC006605 (LOC389389), mRNA*	−7.9	0.1	0.0	0.0	1.6
221655_x_at	*EPS8-like 1*	−7.2	0.1	0.0	0.0	1.5
236058_at	*Hypothetical protein FLJ34633*	−8.8	0.1	0.0	0.0	1.5
225778_at	*RNA binding motif, single-stranded interacting protein 2*	−6.9	0.1	0.0	0.0	1.5
223724_s_at	*DKFZp434A0131 protein*	−6.9	0.1	0.0	0.0	1.5
230111_at	*Transcribed sequence with moderate similarity to protein ref:NP_308425.1*	−7.4	0.1	0.0	0.0	1.5
226095_s_at	*Hypothetical protein LOC146517*	−7.3	0.1	0.0	0.0	1.4
239812_s_at	*Hypothetical protein FLJ12476*	−8.1	0.1	0.0	0.0	1.4
238318_at	*Transcribed sequences*	−7.1	0.0	0.0	0.0	1.2
Genes upexpressed in class 2 PRCC						
201292_at	*Topoisomerase (DNA) IIα, 170 kDa*	6.0	0.4	0.0	0.0	6.5
202920_at	*Ankyrin 2, neuronal*	5.7	0.4	0.0	0.0	5.9
228776_at	*cDNA FLJ40955 fis, clone UTERU2011199*	6.3	0.4	0.0	0.0	4.4
201761_at	*Methylene tetrahydrofolate dehydrogenase (NAD^+ dependent)*	7.7	0.3	0.0	0.0	4.1
209900_s_at	*Solute carrier family 16 (monocarboxylic acid transporters), member 1*	6.7	0.3	0.0	0.0	3.9
218009_s_at	*Protein regulator of cytokinesis 1*	5.6	0.3	0.0	0.0	3.6

(*Continued on the following page*)

Table 3. Top 100 differentially expressed genes in class 1 and 2 PRCC (Cont'd)

Probe ID	Gene description	$D(i)$*	SD	P	Q	Fold change†
202234_s_at	*Solute carrier family 16 (monocarboxylic acid transporters), member 1*	7.1	0.2	0.0	0.0	3.5
209773_s_at	*Ribonucleotide reductase M2 polypeptide*	6.2	0.3	0.0	0.0	3.2
210052_s_at	*TPX2, microtubule-associated protein homologue (Xenopus laevis)*	6.5	0.2	0.0	0.0	3.2
218883_s_at	*KSHV latent nuclear antigen interacting protein 1*	5.5	0.3	0.0	0.0	3.1
225655_at	*Ubiquitin-like, containing PHD and RING finger domains, 1*	5.6	0.3	0.0	0.0	3.1
218039_at	*Nucleolar and spindle-associated protein 1*	6.0	0.3	0.0	0.0	3.0
204822_at	*TTK protein kinase*	5.7	0.2	0.0	0.0	2.9
227607_at	*Associated molecule with the SH3 domain of STAM–like protein*	5.8	0.3	0.0	0.0	2.8
201664_at	*Structural maintenance of chromosomes 4-like 1 (yeast)*	7.8	0.2	0.0	0.0	2.7
201663_s_at	*Structural maintenance of chromosomes 4-like 1 (yeast)*	5.7	0.2	0.0	0.0	2.5
212110_at	*Solute carrier family 39 (zinc transporter), member 14*	5.6	0.2	0.0	0.0	2.5
203554_x_at	*Pituitary tumor-transforming 1*	6.3	0.2	0.0	0.0	2.5
202338_at	*Thymidine kinase 1, soluble*	5.9	0.2	0.0	0.0	2.3
1555758_a_at	*Cyclin-dependent kinase inhibitor 3*	5.8	0.2	0.0	0.0	2.3
202954_at	*Ubiquitin-conjugating enzyme E2*	6.2	0.2	0.0	0.0	2.2
1554408_a_at	*Thymidine kinase 1, soluble*	6.1	0.2	0.0	0.0	2.2
227606_s_at	*Associated molecule with the SH3 domain of STAM–like protein*	5.6	0.2	0.0	0.0	2.1
203764_at	*Discs, large homologue 7 (Drosophila)*	5.9	0.2	0.0	0.0	2.1
221923_s_at	*Nucleophosmin (nucleolar phosphoprotein B23, numatrin)*	5.7	0.2	0.0	0.0	2.0
212295_s_at	*Solute carrier family 7, member 1*	5.4	0.2	0.0	0.0	2.0
204092_s_at	*Serine/threonine kinase 6*	5.6	0.2	0.0	0.0	2.0
202705_at	*Cyclin B2*	5.7	0.2	0.0	0.0	1.9
213188_s_at	*MYC-induced nuclear antigen*	5.8	0.2	0.0	0.0	1.9
228245_s_at	*Ovostatin 2*	6.0	0.2	0.0	0.0	1.9
207828_s_at	*Centromere protein F, 350/400ka (mitosin)*	5.6	0.2	0.0	0.0	1.9
205345_at	*BRCA1-associated RING domain 1*	5.6	0.2	0.0	0.0	1.9
203669_s_at	*Diacylglycerol O-acyltransferase homologue 1 (mouse)*	5.8	0.1	0.0	0.0	1.8
213689_x_at	*Ribosomal protein L5*	5.8	0.1	0.0	0.0	1.7
203562_at	*Fasciculation and elongation protein ζ1 (zygin I)*	5.6	0.1	0.0	0.0	1.7
214096_s_at	*Serine hydroxymethyltransferase 2 (mitochondrial)*	5.4	0.1	0.0	0.0	1.7
205651_x_at	*Rap guanine nucleotide exchange factor 4*	5.4	0.1	0.0	0.0	1.7
213947_s_at	*Nucleoporin 210*	5.7	0.1	0.0	0.0	1.7
230165_at	*Shugoshin-like 2 (Schizosaccharomyces pombe)*	5.4	0.1	0.0	0.0	1.6
218950_at	*ARF-GAP, Rho-GAP, ankyrin repeat and plekstrin homology domain-containing protein 3*	6.5	0.1	0.0	0.0	1.6
203022_at	*RNase H2, large subunit*	6.4	0.1	0.0	0.0	1.5
203719_at	*Excision repair cross-complementing rodent repair deficiency*	6.3	0.1	0.0	0.0	1.5
218115_at	*ASF1 anti-silencing function 1 homologue B (Saccharomyces cerevisiae)*	5.4	0.1	0.0	0.0	1.5
210023_s_at	*Likely orthologue of mouse nervous system polycomb 1*	6.1	0.1	0.0	0.0	1.4
221591_s_at	*Hypothetical protein FLJ10156*	5.6	0.1	0.0	0.0	1.4
204126_s_at	*CDC45 cell division cycle 45-like (S. cerevisiae)*	6.7	0.1	0.0	0.0	1.3
214426_x_at	*Chromatin assembly factor 1, subunit A (p150)*	5.9	0.1	0.0	0.0	1.3
212313_at	*Hypothetical protein MGC29816*	5.9	0.1	0.0	0.0	1.3
221779_at	*Molecule interacting with Rab13*	5.8	0.1	0.0	0.0	1.3
239680_at	*Hypothetical protein FLJ12973*	6.0	0.1	0.0	0.0	1.3

*$D(i)$ is a modified t statistic calculated by SAM.
† Fold change is shown in terms of a relationship between the tumor with higher expression and the tumor with lower expression.

analysis. Ranking of canonical pathways yielded three pathways that were significantly enriched within these differentially expressed genes: G_2-M DNA damage checkpoint regulation (P = 0.007), arginine and proline metabolism (P = 0.011), and G_1-S checkpoint regulation (P = 0.018). Genes involved in G_1-S checkpoint regulation (cyclin D2, cyclin-dependent kinase 6, retinoblastoma-like 2, and $p21^{Cip1}$) were relatively upexpressed in class 1 tumors (Supplementary Fig. S2), whereas genes involved in G_2-M checkpoint regulation (cyclin B1, cyclin B2, and TopIIα) were relatively upexpressed in class 2 tumors (Supplementary Fig. S3). Multiple oligonucleotide probe sets corresponding to c-met were identified as being upexpressed in class 1 tumors, ranging between 2- and 3-fold upexpression. Details of individual gene expression in the 796 transcripts may be found in Supplementary Table S1.

Immunohistochemical characteristics. The immunohistochemical findings are reported in Table 5, and are consistent between the sets of profiled and independent tumors. The majority of class 1 tumors (86%), including type 1 (Fig. 3*A-C*) and type 2A (Fig. 3*D-F*) tumors, showed strong CK7 immunoreactivity (Fig. 3*B* and *E*), whereas the majority of class 2 tumors (Fig. 3*G-L*) showed absent (77%) or reduced (23%) CK7 immunoreactivity in both the set of profiled tumors (Fig. 3*H*) and the independent set of tumors

(Fig. 3*K*). In contrast, TopIIα immunoreactivity was focally positive (10%) or negative (90%) in class 1 tumors, including both type 1 tumors (Fig. 3*C*) and type 2A tumors (Fig. 3*F*). The majority of class 2 tumors were positive for TopIIα (90% positive and 10% focally positive) in both the set of profiled tumors (Fig. 3*I*) and the independent set of tumors (Fig. 3*L*). No TopIIα immunoreactivity was detected in normal kidney tissue. There was no apparent difference between type 1 and low-grade type 2 (type 2A) tumors in CK7 and TopIIα immunostaining. Summarizing the results, CK7 immunoreactivity was significantly higher in class 1 tumors ($P < 0.001$), and TopIIα immunoreactivity was significantly higher in class 2 tumors ($P < 0.001$).

Discussion

Morphologic classification. PRCC is the second most common histologic type of RCC comprising ~10% to 15% of RCC (5) and is composed of tumor cells characteristically forming papillary or tubopapillary structures. The morphologic classification of PRCC into type 1 and 2 tumors has been supported by several histologic studies, although there is relatively limited molecular evidence to substantiate this subtyping. There remains controversy over the recent proposed morphologic classification system of PRCC, preventing its widespread application. For example, there is no agreement whether a tumor with eosinophilic cytoplasm but low nuclear grade should be classified as type 1 or 2. In the initial

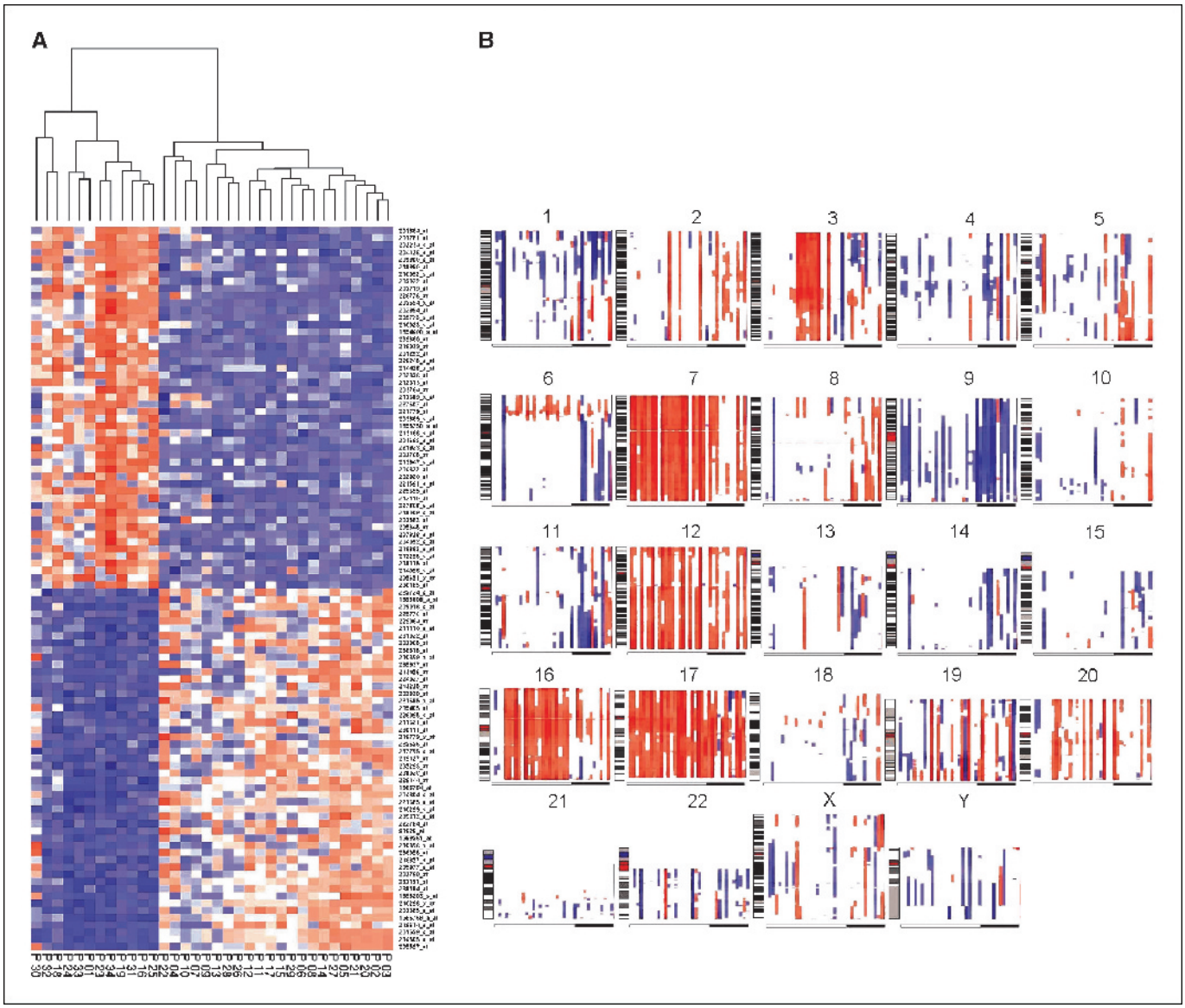

Figure 2. Hierarchical clustering and inferred cytogenetic profiles of class 1 and 2 tumors. *A,* hierarchical clustering of tumor samples by the top 100 differentially expressed genes (50 upexpressed and 50 downexpressed) in each PRCC group. For the heat map: *rows,* individual oligonucleotide probes; *columns,* individual tumor samples; *red,* expression levels greater than the median; *blue,* levels below the median; *white,* levels equal to the median. Complete linkage clustering and a Euclidean distance metric was used, and values were scaled by row. *Left,* group 2 tumors corresponding to all type 2B papillary tumors; *right,* group 1 tumors corresponding to all type 1 and 2A papillary tumors. *B,* CGMA profiles of PRCC were generated from tumor: kidney cortical tissue expression ratios. CGMA shows inferred cytogenetic profiles of the 34 tumor samples. Each block corresponding to a single chromosome represents the chromosomal expression profiles of a group of samples, and each sample is represented by a *single vertical line* in each block. Group 1 tumors correspond to samples above the *white bar*, and group 2 tumors correspond to samples above the *black bar*. *Red bars,* chromosomal regions with a significant number of up-regulated genes (indicating a genomic gain); *blue bars,* chromosomal regions with a significant number of down-regulated genes (indicating a genomic loss). Centromeres are shown in *red* on the chromosomal map to the *left* of each block.

Table 4. Tumor subclass predictor

Probe ID	Gene description	Class 1 score	Class 2 score
232151_at	*mRNA full-length insert cDNA clone EUROIMAGE 2344436*	0.1789	−0.3741
1566766_a_at	*mRNA full-length insert cDNA clone EUROIMAGE 2344436*	0.1419	−0.2967
204304_s_at	*Prominin 1*	0.1182	−0.2472
210298_x_at	*Four and a half LIM domains 1*	0.0164	−0.0342
201539_s_at	*Four and a half LIM domains 1*	0.0159	−0.0332
214505_s_at	*Four and a half LIM domains 1*	0.0101	−0.0211
205597_at	*Chromosome 6 open reading frame 29*	0.0044	−0.0092

NOTE: These class scores are linear discriminant scores for each class as described in the reference for PAM in the text.

proposal outlining this morphologic subtyping (7), 63% of type 2 tumors were assessed as being of low Fuhrman nuclear grade despite pleomorphic nuclei being defined as a characteristic of type 2 tumors. More recently, Allory et al. (26) classified only 1 of 13 (8%) as low-grade type 2 tumors using a modified criteria. The high frequency of tumors with coexisting type 1 and 2 components poses difficulties for such a binary classification, the prevalence of such mixed tumors having been reported as high as 28% (26). Allory et al. chose to classify these tumors with mixed (type 1 and 2) features as type 1 tumors, an approach in line with our molecular classification.

Molecular classification. Our results provide only partial support for the proposed histologic subtyping of PRCC into type 1 and 2 tumors. Type 2 tumors are molecularly heterogenous, with a subset of type 2 (low-grade) tumors and mixed type 1 and 2 tumors demonstrating molecular profiles more consistent with type 1 tumors. These type 2 tumors were all low-grade tumors and showed excellent clinical outcomes, in contrast with the poor outcomes recorded in high-grade type 2 tumors. Type 2 PRCC is composed of at least two genetically distinct subtypes: one subtype (type 2A) resembles type 1 in terms of indolent tumor behavior, excellent survival, low tumor grade, similar expression profiles, immunoreactivity, and inferred cytogenetic profiles; the other subtype (type 2B) is an highly metastatic, aggressive cancer that is molecularly distinct from type 1 or 2A tumors. Our findings support a view that nuclear grade is the key correlate for a molecular classification with both biological and clinical relevance, with features such as cell size or cytoplasmic eosinophilia being more peripheral. Additional distinctive histopathologic features for these subclasses may be defined with a larger series. In this report, the molecular classification showed a statistically insignificant edge in prognostication over the previously proposed histologic classification. However, the molecular approach with correlation to nuclear grade may be more relevant, as it also accurately classifies mixed type 1 and 2 tumors, which are not well accounted for in the histologic classification. This refined classification of PRCC based on both morphologic features and molecular studies may be more relevant and is likely to benefit diagnosis, prognostication, clinical follow-up, and experimental selection of therapeutic targets.

We successfully generated an internally validated seven-transcript predictor, which was able to classify class 1 and 2 tumors with 97% accuracy, the only misclassification arising from a tumor (P30) that we were unable to personally evaluate. Consistent with our microarray classification, this tumor from P30 behaved in an aggressive fashion, the patient relapsing 2 years after surgery. The patient died of a non-cancer-related cause 10 months after relapse. External validation in a second population is required for assessment of true generalizability of these gene predictors, but these results are very encouraging.

Inferred cytogenetic profiles. Aneuploidy is well established as a key driver of global gene expression, and regional DNA copy number correlates well with regional expression in cancer (27), which we have also shown in RCC classification (23). PRCC typically shows frequent trisomies 7, 12, 16, 17, and 20 (5, 28, 29); our analysis is consistent with Fig. 2*A*. For PRCC subclassification, our results are strictly not directly comparable with recent cytogenetic studies that have classified their results by the type 1 and 2 classification (30, 31). As expected, our inferred cytogenetic profiles were consistent with previous studies correlating cytogenetic findings with tumor grade; Lager et al. identifying less

Table 5. Immunohistochemical results

	CK7 immunostaining			TopIIα immunostaining		
	Negative	Focally positive	Positive	Negative	Focally positive	Positive
Profiled tumors						
Type 1	0	0	10	10	0	0
Type 2A	0	0	1	1	0	0
Mixed type 1 and 2A	0	1	2	3	0	0
Type 2B	4	1	0	0	1	4
Independent tumors						
Type 1	0	1	4	5	0	0
Type 2A	1	0	1	0	2	0
Mixed type 1 and 2A	0	0	0	0	0	0
Type 2B	6	2	0	0	0	8
Total	11	5	18	19	3	12

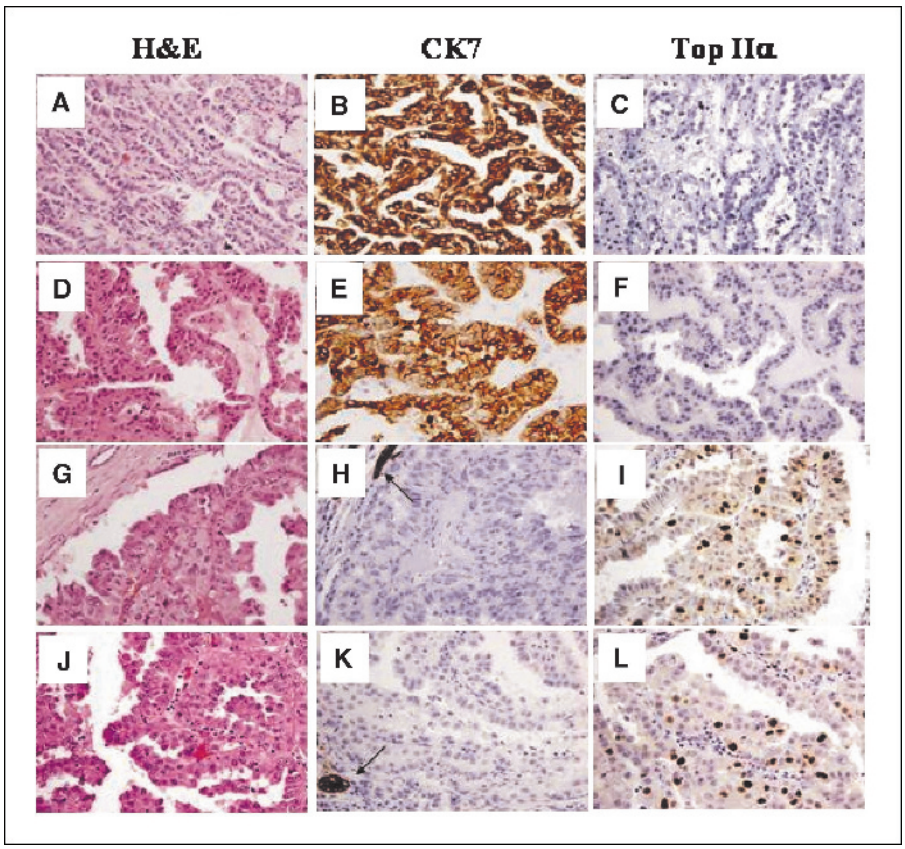

Figure 3. Immunohistochemistry. *A-C,* type 1 tumor was stained with H&E (*A*), CK7 (*B*), and TopIIα (*C*). *D-F,* low-grade type 2 (type 2A) tumor was stained with H&E (*D*), CK7 (*E*), and TopIIα (*F*). *G-I,* high-grade type 2 (type 2B) tumor, which was subjected to microarray analysis, was stained with H&E (*G*), CK7 (*H*), and TopIIα (*I*). Note that a renal tubule (*arrow, H*) stains positive for CK7 as an internal positive control, whereas all tumor cells are negative. *J-L,* high-grade type 2 (type 2B) tumor, which was not subjected microarray analysis, was stained with H&E (*J*), CK7 (*K*), and TopIIα (*L*). Note that a renal tubule (*arrow, K*) is positive for CK7, whereas all tumor cells are negative.

frequent trisomy of 7 in high-grade tumors (32) and Renshaw and Corless reporting that trisomy of 3 was found in a defined subset of low-grade PRCC tumors (33). In addition to these findings, in demonstrating that loss of 9q occurred more commonly in class 2 tumors, our results support a report that loss of heterozygosity at 9q is associated with reduced survival (33).

Immunohistochemical findings. To validate the gene predictor and to derive immunohistochemical markers for the pathology laboratory, we used immunohistochemistry to confirm high protein expression of CK7 in class 1 tumors and of Topo IIα in class 2 tumors. CK7 immunoreactivity has been reported previously to the vast majority of PRCC (33), but more recent studies suggested that CK may differentiate type 1 and 2 tumors. Our microarray and immunohistochemical findings were generally consistent with findings using the morphologic classification that between 87% and 100% of type 1 tumors showed CK7 positivity and ~20% of type 2 tumors showed CK7 positivity (7, 34). No immunohistochemical marker has been reported previously as being specifically upexpressed in type 2 tumors; we showed the usefulness of DNA TopIIα as an immunohistochemical marker in class 2 tumors.

Pathway analysis. Our study highlighted dysregulation of G_1-S checkpoint genes in class 1 PRCC and dysregulation of G_2-M checkpoint genes in class 2 PRCC as the most highly ranked pathways identified in the differentially expressed genes. In familial studies, mutations of the *MET* proto-oncogene have been implicated in hereditary type 1 PRCC (35) and a small subset (<10%) of sporadic type 1 PRCCs (36). Interestingly, we showed that c-met was differentially expressed, with higher expression in class 1 tumors (Supplementary Table S1). From a mechanistic point of view, this associative link between *MET* overexpression/mutation and genes associated with G_1-S checkpoint dysregulation is particularly interesting, as hepatocytes in conditional *met*-mutant mice exhibit defective exit from quiescence and diminished entry into the S-phase of the cell cycle (37). Further work is required to delineate the role of met signaling in G_1-S checkpoint dysregulation. Differential expression of the *FH* gene, which is mutated in a group of families with type 2 PRCC (38), was not observed (data not shown).

The implication of dysregulation of the G_2-M checkpoint regulation in class 2 tumors is particularly interesting from a therapeutic point of view. We took a particular interest in DNA TopIIα, which we additionally established as a diagnostic marker for class 2 tumors. As there is no effective medical therapy for advanced PRCC and this enzyme is associated with the more aggressive PRCC subclass, TopII inhibitors are distinct possibilities for a therapeutic trial of PRCC. G_2 arrest occurs in response to these agents (39) and may therefore be particularly appropriate. Although several kidney cancer trials have reported disappointing results for TopII inhibitors (40, 41), these trials have predominantly recruited patients with clear cell RCC, a genetically distinct disease. In further support of this suggestion, we note that we have reported previously in a microarray study that this gene is the most overexpressed gene in pediatric Wilms' tumor (15), for which current therapeutic regimens consisting primarily of TopII inhibitors are very effective.

Clonal origin versus progression. It has been hypothesized previously based on cytogenetic findings that type 1 tumors progress to type 2 tumors (31). Prudent evaluation of our results in the context of this hypothesis is required. Although microarrays of gross tumor tissue show a global expression signature presumably reflective of early clonal events (42), it is plausible that a competitive growth advantage may accrue to the transformation

of a single cell into a class 2 within a class 1 tumor, resulting in its expansion at the expense of other class 1 tumor cells. Nonetheless, the additional presence of a distinct group of mixed tumors with coexisting type 1 and 2A histology and presenting with molecular profiles resembling other type 1 tumors strongly suggests that type 1 and 2A tumors are clonally more closely related to each other than to type 2B tumors. We did not note the presence of low-grade components in any of our type 2B tumors. Given the divergent survival outcomes following nephrectomy between class 1 (type 1, type 2A, and mixed type 1/2A tumors) and class 2 tumors, we do not favor the idea of progression between class 1 and 2 tumors.

Conclusion

In conclusion, using gene expression profiling supported by immunohistochemical and morphologic studies, we have identified two distinct classes of PRCC that differ strikingly in their clinical behavior and have dysregulation of genes controlling different parts of the cell cycle. This finding represents a biologically and clinically relevant refinement to previously proposed morphologic criteria for subclassification of PRCC. We summarize our findings that may be practically evaluated in the clinical setting laboratory as follows: class 2 (type 2B) PRCC may be distinguished from class 1 (type 1, mixed type 1 and 2A, and type 2A tumors) by the following characteristics: larger gross tumor size, higher nuclear grade (3-4), decreased CK7 staining and increased TopIIα staining, higher rate of metastases at surgery, and poorer patient survival. Morphologic findings of less specificity include larger cell size and eosinophilic cytoplasm in class 2 tumors. Our findings may benefit further efforts to elucidate the molecular basis of development and progression of PRCC and will be helpful in stratifying patients for additional interventions.

Acknowledgments

Received 2/16/2005; revised 3/29/2005; accepted 4/15/2005.

Grant support: Gerber Foundation, Hauenstein Foundation, Fischer Family Trust, and Michigan Technology Tri-Corridor. Four tumor specimens were provided by the Cooperative Human Tissue Network, which is funded by the National Cancer Institute.

The costs of publication of this article were defrayed in part by the payment of page charges. This article must therefore be hereby marked *advertisement* in accordance with 18 U.S.C. Section 1734 solely to indicate this fact.

We thank Dr. Chongfeng Gao for constructive discussion.

References

1. Eble JN, Sauter G, Epstein JI, Sesterhenn IA. Pathology and genetics of tumours of the urinary system and male genital organs. Lyon: IARC Press; 2004.
2. Storkel S, Eble JN, Adlakha K, et al. Classification of renal cell carcinoma: Workgroup No. 1. Union Internationale Contre le Cancer (UICC) and the American Joint Committee on Cancer (AJCC). Cancer 1997;80:987–9.
3. Kovacs G, Akhtar M, Beckwith BJ, et al. The Heidelberg classification of renal cell tumours. J Pathol 1997;183:131–3.
4. Jemal A, Murray T, Ward E, et al. Cancer statistics, 2005. CA Cancer J Clin 2005;55:10–30.
5. Amin MB, Corless CL, Renshaw AA, Tickoo SK, Kubus J, Schultz DS. Papillary (chromophil) renal cell carcinoma: histomorphologic characteristics and evaluation of conventional pathologic prognostic parameters in 62 cases. Am J Surg Pathol 1997;21:621–35.
6. Kuroda N, Toi M, Hiroi M, Enzan H. Review of papillary renal cell carcinoma with focus on clinical and pathobiological aspects. Histol Histopathol 2003;18:487–94.
7. Delahunt B, Eble JN. Papillary renal cell carcinoma: a clinicopathologic and immunohistochemical study of 105 tumors. Mod Pathol 1997;10:537–44.
8. Mejean A, Hopirtean V, Bazin JP, et al. Prognostic factors for the survival of patients with papillary renal cell carcinoma: meaning of histological typing and multifocality. J Urol 2003;170:764–7.
9. Cheville JC, Lohse CM, Zincke H, Weaver AL, Blute ML. Comparisons of outcome and prognostic features among histologic subtypes of renal cell carcinoma. Am J Surg Pathol 2003;27:612–24.
10. Amin MB, Tamboli P, Javidan J, et al. Prognostic impact of histologic subtyping of adult renal epithelial neoplasms: an experience of 405 cases. Am J Surg Pathol 2002;26:281–91.
11. Motzer RJ, Bacik J, Mariani T, Russo P, Mazumdar M, Reuter V. Treatment outcome and survival associated with metastatic renal cell carcinoma of non-clear-cell histology. J Clin Oncol 2002;20:2376–81.
12. Tan MH, Rogers CG, Cooper JT, et al. Gene expression profiling of renal cell carcinoma. Clin Cancer Res 2004;10:6315–21S.
13. Higgins JP, Shinghal R, Gill H, et al. Gene expression patterns in renal cell carcinoma assessed by complementary DNA microarray. Am J Pathol 2003;162:925–32.
14. Takahashi M, Rhodes DR, Furge KA, et al. Gene expression profiling of clear cell renal cell carcinoma: gene identification and prognostic classification. Proc Natl Acad Sci U S A 2001;98:9754–9.
15. Takahashi M, Yang XJ, Lavery TT, et al. Gene expression profiling of favorable histology Wilms tumors and its correlation with clinical features. Cancer Res 2002;62:6598–605.
16. Takahashi M, Yang XJ, Sugimura J, et al. Molecular subclassification of kidney tumors and the discovery of new diagnostic markers. Oncogene 2003;22:6810–8.
17. Young AN, Amin MB, Moreno CS, et al. Expression profiling of renal epithelial neoplasms: a method for tumor classification and discovery of diagnostic molecular markers. Am J Pathol 2001;158:1639–51.
18. Boer JM, Huber WK, Sultmann H, et al. Identification and classification of differentially expressed genes in renal cell carcinoma by expression profiling on a global human 31,500-element cDNA array. Genome Res 2001;11:1861–70.
19. Tretiakova MS, Sahoo S, Takahashi M, et al. Expression of α-methylacyl-CoA racemase in papillary renal cell carcinoma. Am J Surg Pathol 2004;28:69–76.
20. Gentleman RC, Carey VJ, Bates DM, et al. Bioconductor: open software development for computational biology and bioinformatics. Genome Biol 2004;5:R80.
21. Tusher VG, Tibshirani R, Chu G. Significance analysis of microarrays applied to the ionizing radiation response. Proc Natl Acad Sci U S A 2001;98:5116–21.
22. Tibshirani R, Hastie T, Narasimhan B, Chu G. Diagnosis of multiple cancer types by shrunken centroids of gene expression. Proc Natl Acad Sci U S A 2002;99:6567–72.
23. Furge KA, Lucas KA, Takahashi M, et al. Robust classification of renal cell carcinoma based on gene expression data and predicted cytogenetic profiles. Cancer Res 2004;64:4117–21.
24. Jiang Y, Zhang W, Kondo K, et al. Gene expression profiling in a renal cell carcinoma cell line: dissecting VHL and hypoxia-dependent pathways. Mol Cancer Res 2003;1:453–62.
25. Corless CL, Kibel AS, Iliopoulos O, Kaelin WG Jr. Immunostaining of the von Hippel-Lindau gene product in normal and neoplastic human tissues. Hum Pathol 1997;28:459–64.
26. Allory Y, Ouazana D, Boucher E, Thiounn N, Vieillefond A. Papillary renal cell carcinoma. Prognostic value of morphological subtypes in a clinicopathologic study of 43 cases. Virchows Arch 2003;442:336–42.
27. Hughes TR, Roberts CJ, Dai H, et al. Widespread aneuploidy revealed by DNA microarray expression profiling. Nat Genet 2000;25:333–7.
28. Kovacs G, Fuzesi L, Emanual A, Kung HF. Cytogenetics of papillary renal cell tumors. Genes Chromosomes Cancer 1991;3:249–55.
29. Kattar MM, Grignon DJ, Wallis T, et al. Clinicopathologic and interphase cytogenetic analysis of papillary (chromophilic) renal cell carcinoma. Mod Pathol 1997;10:1143–50.
30. Jiang F, Richter J, Schraml P, et al. Chromosomal imbalances in papillary renal cell carcinoma: genetic differences between histological subtypes. Am J Pathol 1998;153:1467–73.
31. Gunawan B, von Heydebreck A, Fritsch T, et al. Cytogenetic and morphologic typing of 58 papillary renal cell carcinomas: evidence for a cytogenetic evolution of type 2 from type 1 tumors. Cancer Res 2003;63:6200–5.
32. Lager DJ, Huston BJ, Timmerman TG, Bonsib SM. Papillary renal tumors. Morphologic, cytochemical, and genotypic features. Cancer 1995;76:669–73.
33. Renshaw AA, Corless CL. Papillary renal cell carcinoma. Histology and immunohistochemistry. Am J Surg Pathol 1995;19:842–9.
34. Ono K, Tanaka T, Tsunoda T, et al. Identification by cDNA microarray of genes involved in ovarian carcinogenesis. Cancer Res 2000;60:5007–11.
35. Schmidt L, Junker K, Weirich G, et al. Two North American families with hereditary papillary renal carcinoma and identical novel mutations in the MET proto-oncogene. Cancer Res 1998;58:1719–22.
36. Schmidt L, Junker K, Nakaigawa N, et al. Novel mutations of the MET proto-oncogene in papillary renal carcinomas. Oncogene 1999;18:2343–50.
37. Borowiak M, Garratt AN, Wustefeld T, Strehle M, Trautwein C, Birchmeier C. Met provides essential signals for liver regeneration. Proc Natl Acad Sci U S A 2004;101:10608–13.
38. Tomlinson IP, Alam NA, Rowan AJ, et al. Germline mutations in FH predispose to dominantly inherited uterine fibroids, skin leiomyomata and papillary renal cell cancer. Nat Genet 2002;30:406–10.
39. Clifford B, Beljin M, Stark GR, Taylor WR. G_2 arrest in response to topoisomerase II inhibitors: the role of p53. Cancer Res 2003;63:4074–81.
40. Escudier B, Droz JP, Rolland F, et al. Doxorubicin and ifosfamide in patients with metastatic sarcomatoid renal cell carcinoma: a phase II study of the Genitourinary Group of the French Federation of Cancer Centers. J Urol 2002;168:959–61.
41. Law TM, Mencel P, Motzer RJ. Phase II trial of liposomal encapsulated doxorubicin in patients with advanced renal cell carcinoma. Invest New Drugs 1994;12:323–5.
42. Ramaswamy S, Ross KN, Lander ES, Golub TR. A molecular signature of metastasis in primary solid tumors. Nat Genet 2003;33:49–54.

A Molecular Classification of Papillary Renal Cell Carcinoma

Ximing J. Yang, Min-Han Tan, Hyung L. Kim, et al.

Cancer Res 2005;65:5628-5637.